INTERNATIONAL JOURNAL OF ENGINEERING SCIENCES & MANAGEMENT

THERMOELECTRIC POWER ENHANCEMENT IN $Pd_xV_2O_5.nH_2O$ HYDRIDE

Samia E. Negm[1], A .S. Abdel Moghny[1], A.S. Abd-Rabo[1], A.A. Bahgat*
Department of Physics, Faculty of Science, Al-Azhar Univ., Nasr City, 11884 Cairo, Egypt

ABSTRACT

$Pd_xV_2O_5.nH_2O$ thin films ($0.00 \leq x \leq 1.094$ mol%) have been prepared using sol gel dip coating technique. X-ray diffraction (XRD), thermogravimetric analysis (TGA), thermoelectric power (S) and electrical conductivity (σ) of $Pd_xV_2O_5.nH_2O$ thin films fabricated by sol gel technique (colloid route) were studied in air and hydrogen. H-$Pd_xV_2O_5.nH_2O$ thin films exhibit a change in their structural, thermal and electrical properties when exposed to hydrogen. Our results showed that the thermoelectric performance of the $Pd_xV_2O_5.nH_2O$ thin films has been enhanced when measured in hydrogen rather than in air by percentage ranging between 1.2 to about 35%.

KEYWORDS: A. thin films; B. sol-gel growth; C. thermogravimetric analysis (TGA); D. transport properties.

INTRODUCTION

Growing energy demands, concerns over climate change and depletion of fossil fuel resources have led to a concerted effort to develop sustainable technologies for the efficient use, conversion, and recovery of energy. One such technology is the use of thermoelectric (TE) materials to directly convert heat into electricity, based on the Seebeck effect, which was discovered in 1836 by Thomas Johann Seebeck. It should be noted that TE materials can also convert electricity into cooling through the Peltier effect [1, 2]. This technology has distinct advantages, including:

1) TE conversion is reliable and operates in silence compared with other energy conversion technologies, as it works without mechanical movement.
2) TE devices are simple, compact, and safe.
3) It is an environmentally friendly green technology, because no heat and no gaseous or chemical waste are produced during operation.
4) It can be widely used in places where other energy conversion technologies are unavailable, such as in the remote outer space [1].

There are three different thermoelectric effects [3]:

- The Seebeck effect: When two junctions of different metals are placed at temperature difference ΔT, a voltage ΔV will develop. The Seebeck coefficient is defined as:

$$S = lim_{\Delta T \to 0} \frac{\Delta V}{\Delta T} \qquad (VK^{-1}) \qquad (1)$$

- The Peltier effect: When a current I is passed through a junction between two different conductors, heat Q is absorbed or released depending on the direction of the current. The Peltier coefficient is defined as:

$$\Pi = Q/I \qquad (WA^{-1}) \qquad (2)$$

- The Thomson effect: When a current I is passed through a homogeneous conductor with a temperature gradient ΔT, a heating or cooling effect ΔQ is shown.
  The Thompson coefficient is defined as:

$$\gamma = lim_{\Delta T \to 0} \frac{\Delta Q}{I \Delta T} \qquad (WA^{-1} K^{-1}) \qquad (3)$$

Materials suitable for thermoelectric applications fall mainly into two categories: semiconductors and mixed-valent compounds, although some semimetals may also be viable [4].

For semiconductors, the best materials have the following properties:

- Electronic bands near the Fermi level, with many valleys, preferably away from the Brillouin zone boundaries. This requires high symmetry.
- Elements with large atomic number and large spin-orbit coupling.
- Compositions with more than two elements (i.e., ternary, quaternary compounds).
- Low average electronegativity differences between elements.
- Large unit cell sizes.
- Energy gaps equal to 10 k_BT, where T is the operating temperature of the thermoelectric material.

These basic criteria, if satisfied, should give rise to high carrier mobility, low thermal conductivity and large thermoelectric power [4].

Vanadium pentoxide V_2O_5, which crystallizes in a layered structure, has been widely used in a variety of scientific and technological applications. It can be used as a catalyst, as a gas sensor, as a cathode for solid-state batteries, as windows for solar cell and for electrochromic devices as well as for electronic and optical switches [5]. Bahgat et al. [6] studied the highly oriented $V_2O_5.nH_2O$ nanocrystalline film with excellent properties prepared by the sol-gel technique. In this study XRD as well as transmission electron microscope (TEM) and electron diffraction measurements showed that $V_2O_5.nH_2O$ is highly oriented nanocrystals. Extended gate field effect transistor using V_2O_5 xerogel sensing membrane by sol-gel method had been studied by Guerra et al [7]. The X-ray diffractogram showed that the V_2O_5 xerogel is a lamellar character and the surface of the film showed the presence of agglomerates, fibrils and ribbons along a direction parallel to substrate [7, 8]. The film was investigated as a sensor in the pH range 2-12 and the corresponding Extended Gate Field Effect Transistor (EGFET) has a sensitivity of 58.1 mV/pH. This value suggests that the material is a promising candidate for applications as disposal biosensor .

It is commonly known that at temperatures above 10 K molecular hydrogen dissociates on the surface of transition metals. Under appropriate conditions hydrogen interaction with transition or rare earth metals leads to new compounds M-H_x hydrides. Metal hydrides are nonstoichiometric compounds with hydrogen distributed along the interstitial sites of the metal, held in place by a combination of covalent and ionic bonding [9]. Metal hydrides are created when equilibrium hydrogen pressure P_{eq} characteristic of M-H_x is exceeded. Hydrogen is an element which has the ability to lose or accept an electron, thus becoming a proton or forming a negative ion of the stable configuration of a helium atom. Experimental results collected in the literature show that both states of hydrogen can be present on the surface and also in the bulk of various metals. H^- anions are present without any doubt in hydrides of alkaline metals [9], whereas it has been experimentally proved that in the bulk of hydrides of several transition metals e.g. palladium, niobium or vanadium, hydrogen is clearly protonic [9].

On the other hand, the simplest hydrogen sensors are based on monitoring changes in electrical properties of group VIII transition metals, especially palladium (Pd). Hydrogen adsorbs on Pd surface and diffuses into its bulk altering its electrical and optical properties. This variation is used to detect/estimate hydrogen in the ambiance. However, at high hydrogen concentrations palladium undergoes a phase change. This causes an expansion of the lattice – a problem for fabricating reliable sensors using this metal [10].

The main objective of the present work is to investigate the thermoelectric power TEP & power factor TPF of $Pd_xV_2O_5.\ nH_2O$ hydride.

Experimental

Six different compositions of $Pd_xV_2O_5.nH_2O$ (where x = 0.00, 0.219, 0.438, 0.656, 0.875 and 1.094 mol%) have been prepared for the present investigation. Films of the investigated compounds were prepared by sol-gel technique (colloidal route). Generally, several methods may be followed to prepare $V_2O_5.nH_2O$ xerogel [5, 11]. Typically, the most simple and cost effective methods are either by dissolving V_2O_5 in hydrogen peroxide H_2O_2 [6, 12, 13] or by pouring V_2O_5 melt at 800^{o}C in continually stirred distilled water [14, 15]. Both routes produce xerogels of similar atomic structure, however they may show different properties when compared with analogous series of samples *e.g.:* $Li_xV_2O_5.nH_2O$ [11].

In the present study, films of the investigated compounds were prepared by dip and flow coating sol-gel technique (colloidal route). The powder of vanadium pentoxide (V_2O_5) (99.99%) and palladium chloride, $PdCl_2$ - 99.9% *(SIGMA-ALDRICH)* in suitable proportions (mol%) were used as raw materials. A batch of (1.0185 g) of V_2O_5 was dissolved in 80 ml of 17.5% hydrogen peroxide (H_2O_2) at room temperature. The formed solution was stirred continuously using magnetic stirrer. The solution was then heated at 60 ^{o}C, with uninterrupted continuous stirring while the pH was kept in the range 2-3. Further increase of the pH would wipe out the gel formation and the process would stop. Acetic acid-dissolved $PdCl_2$ (0.426 g) was added to the V_2O_5 gel drop by drop using a Pruitt up to the desired concentration, while keeping the pH not to exceed 3. Vanadium pentoxide (V_2O_5) and (V_2O_5-(x) $PdCl_2$) gels can be synthesized via the condensation of aqueous solutions. The obtained gels were deposited on Pyrex substrate by dip and flow coating techniques. The samples were made in coplanar geometry and dried spontaneously in air to orient the layered plane. The structure of thin films prepared by sol-gel technique was studied by X-ray diffraction

supplies with a copper target and Ni filter producing X-ray with wavelength equal to 1.5418 Å. The diffraction patterns were recorded automatically in the angular range $2\theta = 4\text{-}90^{o}$ with a step of 0.02^{o}. The thermal behaviors of the prepared samples were studied using TGA & DSC techniques. TGA curves of the $Pd_xV_2O_5.nH_2O$ system with $0.00 \leq x \leq 1.094$ mol% were measured using SDT Q600 V20.5 Build 15 (Universal V4.5A TA Instruments). Generally, TGA is commonly used to determine selected characteristics of materials that exhibit either mass loss or gain due to decomposition, oxidation, or loss of volatiles (such as moisture) due to thermal treatment. On the other hand, the dc electrical conductivity σ_{dc} was measured in the temperature range of 340 - 460 K by the two probe method using silver painted electrodes. The thermoelectric power, TEP, on the other hand of the samples was measured between two Cu-electrodes and two K-type thermocouples attached to the samples. Different measurements were done in air and 100% hydrogen, respectively.

RESULTS & DISCUSSION

X-ray diffraction (XRD)

X-ray diffraction, XRD, patterns were obtained in order to study the structure and the particle size of the prepared under test films in air and hydrogen. These patterns for the $Pd_xV_2O_5.nH_2O$ thin films as synthesized by the Sol-gel technique on a glass substrate are shown in Fig. 1a-f. The XRD patterns of the films show the [001] peak at about $2\theta = 8.304^{o}$ indicating a high preferential c-axis orientation and is a characteristic of the one dimensional stacking of the vanadium pentoxide xerogel ribbons perpendicular to the substrate surface while vanadium-oxygen layers are formed by tangled fibers and connected by water molecules [12, 16]. Fig. 1a-f shows that all patterns demonstrate the same overall features indicating that the structure of the films remains unaltered by the intercalation of Pd^{+2} ions, but when samples have been exposed to hydrogen atmosphere producing $H\text{-}Pd_xV_2O_5.nH_2O$ hydride a shift in the [001] peak has been observed as well as an enormous drop of the intensity as shown in Fig. 1a-f. A relation between the composition and shift in [001] pattern due to measurement in air and hydrogen is indicated in Fig.2a.

The crystallite size (grain size), D, of these films estimated using Scherer's formula [17]:

$$D = 0.94\,\lambda / \beta \cos\theta \qquad (4)$$

where β is full width at half maximum, FWHM, in radian of XRD yields, λ is the X-ray wavelength and θ is the Bragg's angle. The dislocation density, δ, of thin film is given by the relation [18];

$$\delta = n/D^2 \qquad (5)$$

where n is a factor, which is unity. The obtained results are given in Table 1 and presented in Fig. 2b&c.

In summary, Fig.1 shows that the lamellar structure is maintained after intercalation process. The analysis revealed that Pd^{+2} are intercalated within V_2O_5 layers, without almost any change in the structure to form $Pd_xV_2O_5.nH_2O$ system. An obvious shift in [001] peak while exposing $Pd_xV_2O_5.nH_2O$ thin films to hydrogen producing $H\text{-}Pd_xV_2O_5.nH_2O$ hydride as shown in Fig.1(a-f) & Fig 2(b&d). Hydrogen is dissociated on the surface of $Pd_xV_2O_5.nH_2O$ thin film and hydrogen atoms diffuse to the interface between palladium and vanadium oxide. A high average vanadium oxidation state enhances the absorption of hydrogen in two aspects: a low chemical potential that results in a high thermodynamic driving force, and a large capacity to react with hydrogen due to the great amount of vanadium (V) species that can be reduced [19]. The presence of a vanadium oxide layer that is capable of accepting hydrogen allows the palladium hydride layer to be stable.

Table 1: X-ray structural data for the system $Pd_xV_2O_5.nH_2O$, where d_{001} is the interlayer spacing, D is the average particle size and δ is the dislocation density.

x mol%	Air			Hydrogen			I_H/I_A
	D (nm)	d_{001} (nm)	δ ($nm^{-2}\times10^{-3}$)	D (nm)	d_{001} (nm)	δ ($nm^{-2}\times10^{-3}$)	
0.000	12.49	1.092	6.25	11.54	1.075	7.51	0.826
0.219	13.75	1.135	5.29	19.32	1.074	2.68	0.813
0.438	15.45	1.191	4.19	20.61	1.070	2.35	0.514
0.656	21.46	1.21	2.17	-	-	-	0.129
0.875	26.65	1.19	1.41	32.20	1.066	0.97	0.277
1.094	31.53	1.177	1.02	38.66	0.934	0.67	0.181

Thermogravimetric analysis (TGA)

Thermal properties of $Pd_xV_2O_5.nH_2O$ films with $0.000 \leq x \leq 1.094$ mol% were studied by thermogravimetric analysis (TGA). Thermogravimetric properties of the $Pd_xV_2O_5.nH_2O$ films were investigated by thermogravimetric analysis from room temperature to 600 °C in air at a heating rate of 2° C min^{-1} and the results are shown in Fig.3.

In this research the 10.18% weight loss below 250 °C for samples measured in air can mainly be ascribed to the loss of weakly bound water, and the weight loss between 250 °C and 340 °C generally involves the loss of crystallization water from $Pd_xV_2O_5 \cdot nH_2O$, whereas above 340°C the formation of V_2O_5 phase occurs [16]. For the samples exposed to hydrogen, Fig. 3 shows that there's a difference in TGA curves for samples measured in air and as exposed to hydrogen prior to the measurements. Difference is due to the interaction between Pd ions and hydrogen molecules producing palladium hydride.

$$Pd(s) + n/2\ H_2(g) \rightarrow PdH_n(s)$$

Palladium hydride has different thermal properties from those exposed to air. Looking to Fig.3 the weight loss of $Pd_xV_2O_5 \cdot nH_2O$ is different from that H-$Pd_xV_2O_5 \cdot nH_2O$ hydride. Weight loss below 250°C and that between 250 °C and 400 °C attributed to the loss of water molecules interacted with hydrogen molecules as shown in Fig.3. As shown in Fig.3, weight loss below 250°C for $Pd_xV_2O_5 \cdot nH_2O$ ranging between 2.25 to about 6%, while for H-$Pd_xV_2O_5 \cdot nH_2O$ hydride it reached to about 10%.

Thermoelectric power (S) & electrical conductivity (σ)

Electrical conductivity (σ) and thermoelectric power (S) were measured for $Pd_xV_2O_5.nH_2O$ thin films as a function of temperature in the temperature range 303 to 453 K in air and hydrogen. Thermoelectric power of hydrogenated H-$Pd_xV_2O_5.nH_2O$ show enhancement in the temperature range 303 to about 380 K. Moreover, the power factor which is used to measure the energy conversion efficiency has been enhanced in hydrogenated $Pd_xV_2O_5$, nH_2O. The definition of power factor is [20]:

$$TPF = S^2\sigma \qquad (6)$$

Enhancement of thermo power factor means enhancing the Seebeck coefficient *S*, the electrical conductivityσ or both.

Fig.4 shows the temperature dependence of electrical conductivity (σ), thermoelectric power (S) and power factor (TPF) for $Pd_xV_2O_5.nH_2O$ and hydrogenated H-$Pd_xV_2O_5$. nH_2O. Hydrogenated H-$Pd_xV_2O_5.nH_2O$ possess some high-efficient thermoelectric characteristics within low temperatures. Hydrogenated $Pd_xV_2O_5.nH_2O$ showed improved TEP performance than $Pd_xV_2O_5$. nH_2O.

On the other hand the sign of the thermoelectric power is found to be negative which indicates that the conduction takes place due to electrons in the conduction band. Hence the samples under test are n-type semiconductor as observed in Fig. (5b).

Early studies on binary V_2O_5-P_2O_5 glasses, based on EPR studies and wet chemical analysis, indicated that the relative abundance of vanadium in V^{4+} valance state $\left(C = \frac{[V^{4+}]}{[V^{4+} + V^{5+}]} \right)$ is a decreasing function of V_2O_5 content in a glass [21, 22]. Thermoelectric power measurements were used to determine ***C***. It has been demonstrated that the thermoelectric power of vanadate glasses depend only on the ratio of high to low valance state of vanadium and obey the relationship [23]:

$$S = \frac{k_B}{e} \ln\left(\frac{C}{1-C}\right) \qquad (7)$$

On the other hand, the ratio of low to high valancy state of vanadium may be determined by, ESR, and chemical analysis as well. The obtained values of ***C*** values are shown for $Pd_xV_2O_5.nH_2O$ and $Pd_xV_2O_5.nH_2O$ hydride in Fig. (5a) as a function of ***x***.

The temperature independence of TEP (at room temperature and above) reveals that all available V^{4+} ions are active centers, and therefore all are taking part in to the conduction. Similar results were obtained previously for the pure V_2O_5 xerogel [11] and in $K_xV_2O_5.nH_2O$ gel [24]. This present result (*S* in the range -120 to -90 μV/K; when *C*=0.10) is explained in spite of the complicated structure of xerogels, as the conduction mechanism is still through V_2O_5 ribbons by small polaron hopping among V^{4+} and V^{5+} sites [25]. Consequently, the similarity in the transport properties of glasses and xerogels would not be surprising. Amorphous semi- conductors in general demonstrate an electronic conduction, whereas V_2O_5 glasses or xerogels are polaronic materials [25]. As shown in Fig.5a, the value of *C* increases as the Pd^{2+} ions content increases (*i:e:* decreasing the amount of V^{5+}). This may be understood if the conservation of the overall charge neutrality of the system is considered, the crystal structure is preserved, as presented from the XRD results.

Fig.5c shows the composition dependence of thermopower factor (TPF) & its percentage of enhancement while measuring $Pd_xV_2O_5.nH_2O$ in H_2 producing $Pd_xV_2O_5.nH_2O$ hydride.

Kounavis et al, have demonstrated that V_2O_5 gels exhibit a room temperature TPF of 0.3 $\mu W/mK^2$ [26]. V_2O_5 films synthesized by sol gel method exhibit S of ~ 200 μV/K, but have a very high resistance of $10^3 - 10^4$ Ω [16, 25]. Hence it is evident that the (σ) of V_2O_5 films requires significant enhancement for practical refrigeration and energy scavenging applications [27].

H-$Pd_xV_2O_5.nH_2O$ hydride thin films appeared a good enhancement in TEP & TPF in the temperature range 303 to about 400 K which is a region of importance for practical application particularly in space.

CONCLUSION

Highly oriented $Pd_xV_2O_5.nH_2O$ ($0.00 \leq x \leq 1.094$ mol %) nanocrystalline thin films have been prepared using sol gel technique. XRD, TGA, electrical conductivity and thermoelectric power has been measured in air and hydrogen. $Pd_xV_2O_5.nH_2O$ thin films exhibit a change in their structural, thermal and electrical properties when exposed to hydrogen. Our results show that the thermoelectric performance of the $Pd_xV_2O_5.nH_2O$ thin films has been enhanced when measured in hydrogen rather than in air by percentage ranging between 1.2 to about 35%. An enhancement in thermopower factor has been observed in $Pd_xV_2O_5,.nH_2O$ hydride in percentage between 10 to 75 % in the temperature range 303 to 400 K.

REFERENCES

1. Chao Han, Zhen Li and Shixue Dou, Chin. Sci. Bull. 59(14) (2014) 2073-2091.
2. Jin-Cheng ZHENG, Front. Phys. China, 3(3) (2008) 269-279.
3. G.M. Gonzalez, R. Rodriguez-Mijango and G.Vazquez-polo, Revista Mexicana DE Fisica 51(6) (2005) 633-635.
4. Michael Constantine Nicolaou, *"Thermoelectric Figure of Merit of Degenerate and non degenerate Semiconductors"*, PhD thesis, North Eastern University Boston, Massachusetts 2008.
5. J. Livage, Coord. Chem. Rev. 190-192 (1999) 391.
6. A.A. Bahgat, F.A. Ibrahim, M.M. El-Desoky, Thin. Solid. Films. 489 (2005) 68.
7. Elidia Maria Guerra, Glaucio Ribeiro Silva and Marcelo Mulato, Solid State Sciences, 11 (2009) 456.
8. V. Petkov, P.N. Trikalitis, E.S. Bozin, S.J.L. Billinge, T. Vogt, M.G. Kanatzidis, J. Am. Chem. Soc. 124 (2002) 10157.
9. R. Dus, E. Nowicka and R. Nowakowski, Acta Physica Polonica A, 114 (2008) S-29 – S-49.
10. Raviprakash Jayaraman, *"Thin film hydrogen sensors: Materials processing approach"*, PhD thesis, 2002.
11. M.S. Al-Assiri, M.M. El-Desoky, A. Alyamani, A. Al-Hajry, A. Al-Mogeeth and A.A. Bahgat: *Philos.Mag.*, 90(25) (2010) 3421.
12. S.E. Negm, H.A. Mady, A.S. Abdel Moghny, A.S. Abd-Rabo and A.A. Bahgat: *Solid State Sci.*, 13 (2011) 590.
13. G.T. Chandrappa, N. Steunou, S. Cassaignon, C. Bauvais and J. Livage: *Catal. Today*, 78 (2003) 85.
14. N. Ozer: Thin Solid Films, 305 (1997) 80.
15. Z.S. El Mandoh and M.S. Selim: Thin Solid Films, 371 (2000) 259.
16. Samia E. Negm, A.S. Abdel Moghny, A.S. Abd-Rabo, A.A. Bahgat, Journal of Applied Sciences Research, 9(11) (2013) 5756-5761.
17. E.M. Guerra, G.R. Silva, M. Mulato, Solid State Sci. 11 (2009) 456.

18. G.K. Willianson, W.H. Hall, Acta. Metal. 1 (1) (1953) 22.
19. D.Smith II, Ping Liu, See-Hee Lee, C.Edwin Tracy and J.Roland Pitts, 47(2) (2002) 826.
20. S. Walia, S. Balendhran, H. Nili, S. Zhuiykov, G. Rosengarten, Q. Hua Wang, M. Bhaskaran, S. Sriram, M.S. Strano, K. Kalantar-zadeh, Progress in Materials Science 58(8) (2013) 1443–1489.
21. V. Bondarenka and A. Pasiskevicius, J. Physics, 46 (2006) 283.
22. K. Honma, M. Yoshinaka, K. Hirota and O. Yamaguchi, J. Mat. Res. Bull., 31 (1996) 531.
23. Abdulaziz Mohammed, M.Sc. thesis, King Khalid University, KSA, 2007.
24. Y.J. Liu, J.A. Cowen, T.A. Kplan, D.C. De Groot, J. Schindler, C.R. Kannewurf and M.G. Kanatzidis: *Chem. Mater.*, 7 (1995) 1616.
25. A.A. Bahgat, H.A. Mady, A.S. Abdel Moghny, A.S. Abd-Rabo and Samia E. Negm, J. Mater. Sci. Technol., 27(10) (2011) 865- 872.
26. Kounavis P, Vomvas A, Mytilineou E, Roilos M, Murawski L. J.Phys C – Sol State Phys 21(1988) 967–973.
27. Sumeet Walia, Sivacarendran Balendhran, Hussein Nili, Serge Zhuiykov, Gary Rosengarten, Qing Hua Wang, Madhu Bhaskaran, Sharath Sriram, Michael S. Strano and Kourosh Kalantar-zadeh, Progress in Materials Science 58 (2013) 1443–1489.

ISSN: 2277-5528
Impact Factor: 2.745 (SIJF)

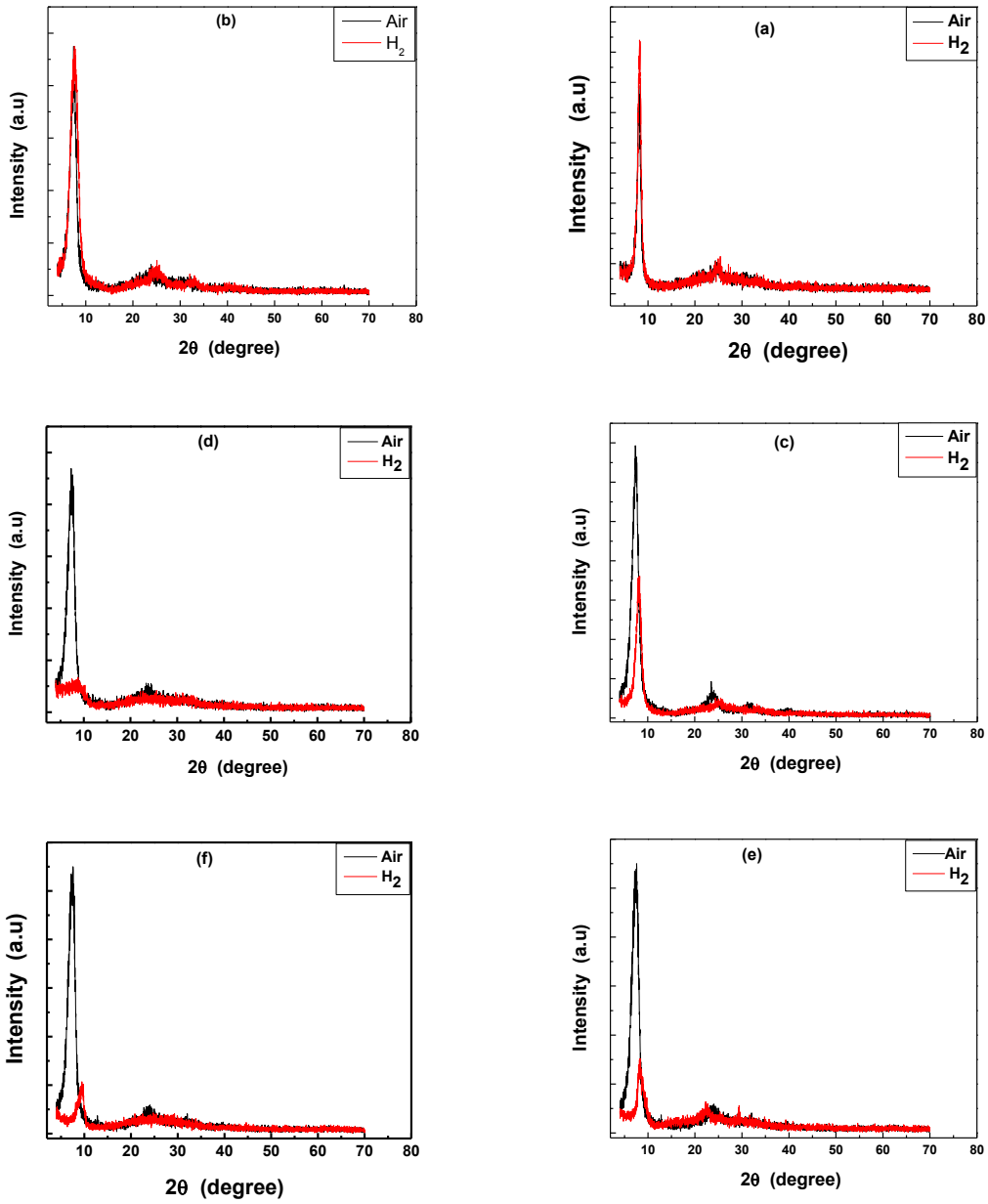

Fig. 1. Room temperature X-ray diffraction for the nanocrystalline system $Pd_xV_2O_5.nH_2O$ in air & H_2 with x (a = 0.000, b = 0.219, c = 0.438, d = 0.656, e = 0.875, f = 1.094) in mol%.

ISSN: 2277-5528
Impact Factor: 2.745 (SIJF)

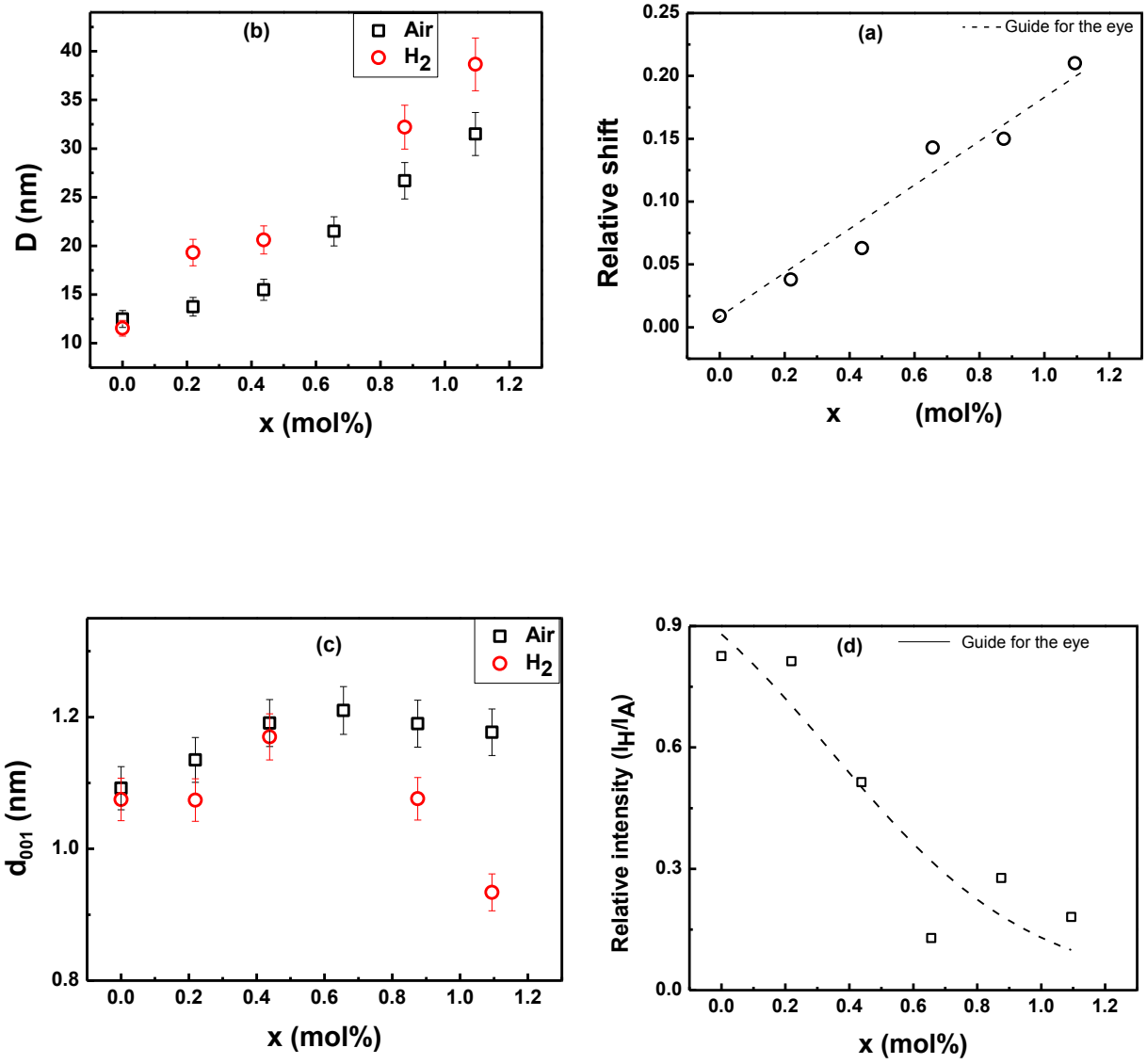

Fig. 2. X-ray results, (a) the relative shift of 001 peak between patterns measured in air & H_2., (b) particle size D for the nanocrystalline $Pd_xV_2O_5.nH_2O$ sol-gel system and (c) lattice constant d_{001}.

ISSN: 2277-5528
Impact Factor: 2.745 (SIJF)

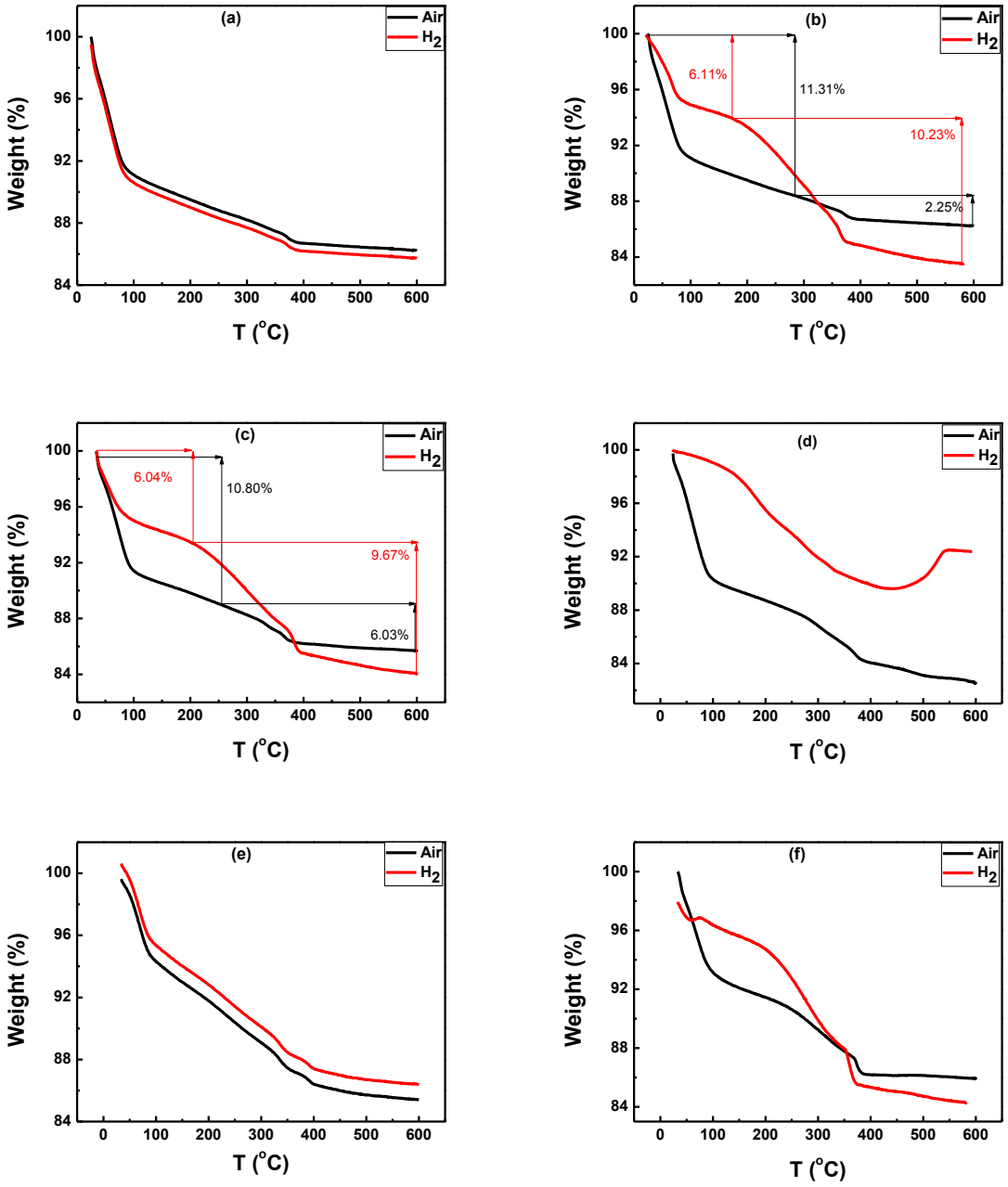

Fig. 3. Thermogravimetric analysis (TGA) of $Pd_xV_2O_5.nH_2O$ films air & H_2 with x (a = 0.000, b = 0.219, c = 0.438, d = 0.656, e = 0.875, f = 1.094) in mol%.

ISSN: 2277-5528
Impact Factor: 2.745 (SIJF)

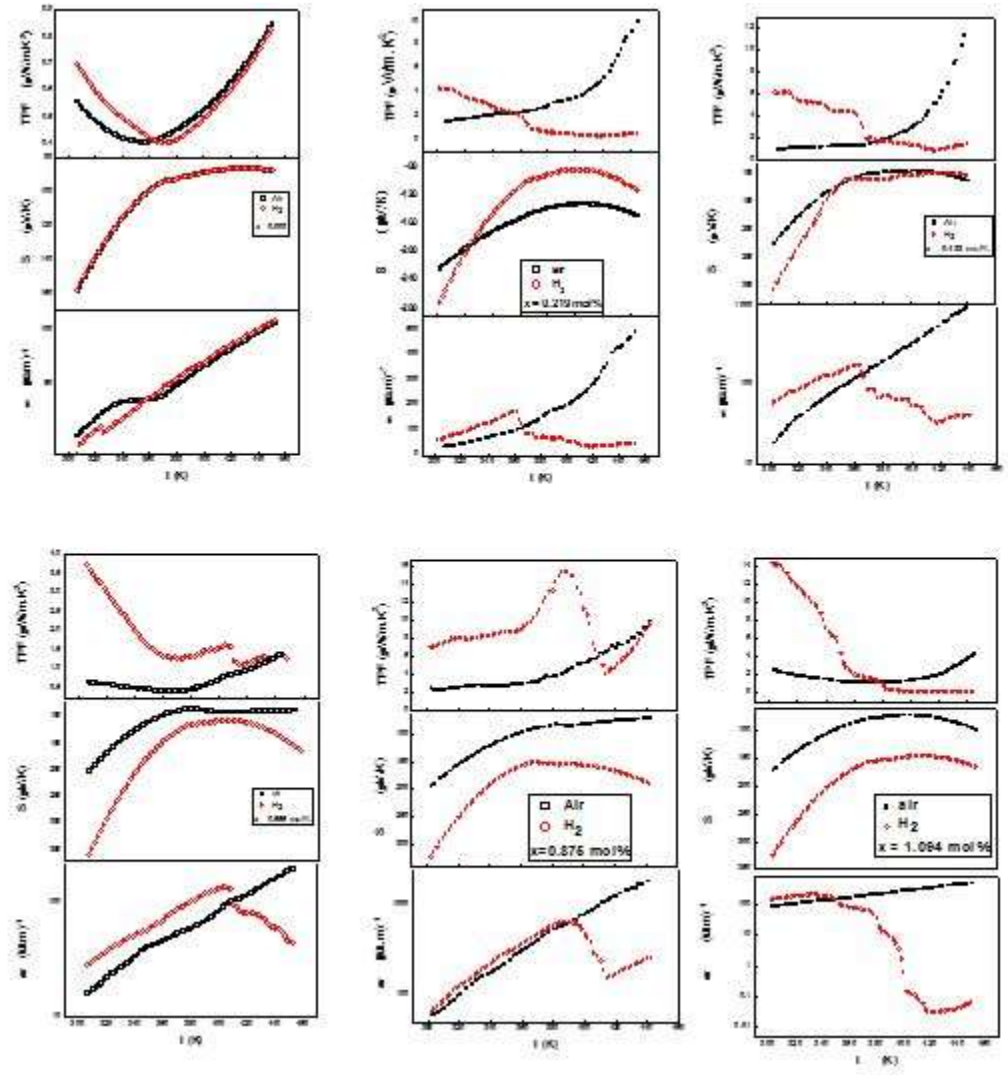

Fig.4. Electrical conductivity σ, thermoelectric power S and TPF of $Pd_xV_2O_5.nH_2O$ system as measured in air & hydrogen for.

ISSN: 2277-5528
Impact Factor: 2.745 (SIJF)

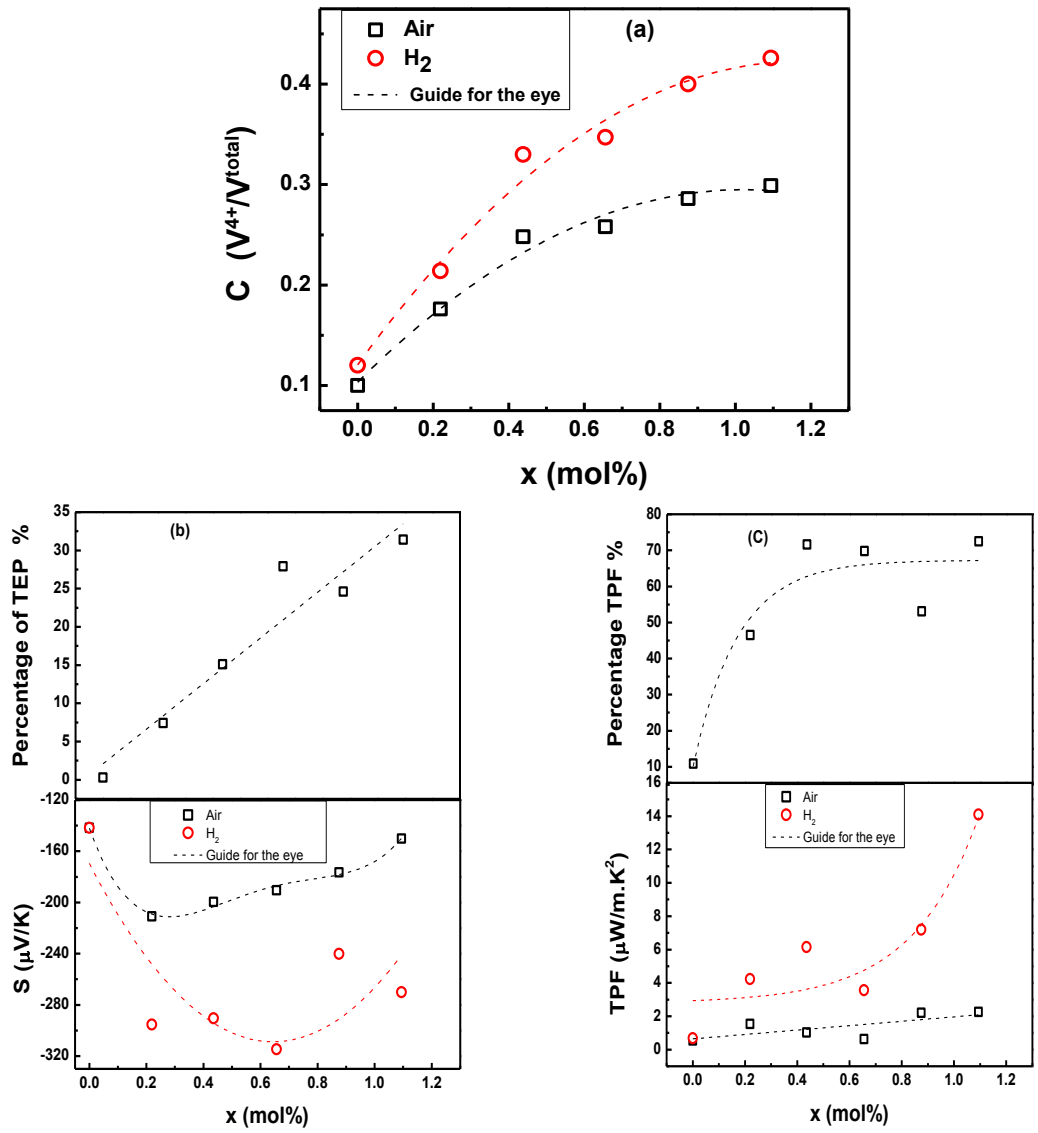

Fig.5. The composition dependence of (a) C values of $Pd_xV_2O_5.nH_2O$ in air and H_2, (b) TEP of $Pd_xV_2O_5$. nH_2O in air and H_2 & its relative enhancement and (C) TPF of $Pd_xV_2O_5.nH_2O$ in air and H_2 & its relative enhancement.